Self-organization of magnetic moments in dipolar chains with restricted degrees of freedom

Alexander F. Pshenichnikov and Andrey A. Kuznetsov
Laboratory of Dynamics of Dispersed Systems, Institute of Continuous Media Mechanics UB RAS, Korolyov Street 1, Perm 614013, Russia
(Received 6 July 2015; published 6 October 2015)

Equilibrium behavior of a single chain of dipolar spheres is investigated by the method of molecular dynamics in a wide range of the dipolar coupling constant λ. Two cases are considered: rodlike and flexible chains. In the first case, particle centers are immovably fixed on one axis, but their magnetic moments retain absolute orientational freedom. It has been found that at $\lambda \gtrsim 1.5$ particle moments are chiefly aligned parallel to the chain axis, but the total moment of the chain continuously changes its sign with some mean frequency, which exponentially decreases with the growth of λ. Such behavior of the rodlike chain is analogous to the Néel relaxation of a superparamagnetic particle with a finite energy of magnetic anisotropy. In the flexible chain particles are able to move in the three-dimensional space, but the distance between centers of the first-nearest neighbors never exceeds a given limiting value $r_{\max}$. If $r_{\max} \simeq d$ (d is the particle diameter) then the most probable shape of the chain of five or more particles at $\lambda \gtrsim 6$ is that of a ring. The behavior of chains with $r_{\max} \geqslant 2d$ is qualitatively different: At $\lambda \simeq 4$ long chains collapse into dense quasispherical globules and at $\lambda \gtrsim 8$ these globules take toroidal configuration with a spontaneous azimuthal ordering of magnetic dipoles. With the increase of $r_{\max}$ to larger values ($r_{\max} > 10d$) globules expand and break down to form separate rings.

DOI: 10.1103/PhysRevE.92.042303 PACS number(s): 62.23.St, 75.50.Mm, 75.75.Jn

I. INTRODUCTION

One of the distinguishing features of single-domain nanoparticles placed in a viscous medium is their ability to form chain aggregates, inside which the magnetic moments of adjacent particles are ordered in a "head-to-tail" manner. The aggregation phenomenon is a direct consequence of the anisotropic nature of dipole-dipole interactions. Its theoretical understanding was developed in the classical paper by de Gennes and Pincus [1]. The authors investigated the behavior of particles in a dilute magnetic fluid (MF) and showed that in zero magnetic field these particles can be arranged into arbitrarily oriented chains, clusters, and ring-shaped aggregates. In the applied field the probability of chain formation increases and chains align themselves with magnetic field lines. Later, the existence of chains in MF was substantiated by the results of laboratory [2] and numerical experiments [3–8]. The presence of chain aggregates can significantly influence hydrodynamic, magneto-optic, and rheological properties of MF [9], which gave an impetus to a great number of theoretical studies devoted to chains [10–20]. The problem of chain structures also arises in tackling the phenomenon of MF phase separation.

Phase separation of MF was predicted in Ref. [1] and was interpreted as a result of dipole-dipole interactions, which after being averaged over dipole orientations lead to an effective attraction between particles. Phase separation accompanied by the formation of condensed phase drops amid the rarefied "gas" of colloidal particles was repeatedly observed in laboratory experiments both in the presence and absence of the applied magnetic field [21]. In the light of these findings, new numerical results obtained in early 1990s came as a complete surprise to many researchers. They evidenced against the existence of the "gas–liquid" phase transition in the systems of hard and soft dipolar spheres, i.e., in the simplest MF models that take into account only steric and magnetodipole interparticle interactions [3,4,22,23]. Instead of the phase separation taking place at decreasing temperatures and low particle concentrations, the researchers observed the formation of a dipolar chain "gel." Theoretical studies that appeared at that time showed that a tendency of particles to aggregation competes with the tendency to condensation and indeed can suppress the phase transition [11,12]. A recent series of papers Ref. [24], where high-precision Monte Carlo simulation was combined with analytical studies, also lend support to the view that in a potential transition zone the system of hard dipolar spheres in fact maintains the spatial homogeneity while being in a highly aggregated state. Chains and rings in the system coexist with branching structures, and with decreasing particle concentration rings become dominant. It is worth noting that in some works on numerical simulation signs of the phase separation have been observed, but these works are fewer in number [25–27]. In Refs. [19,20] authors suggested that phase separation in the aggregated system might still occur through the collapse of the longest chains into compact globular structures, which act as condensation nuclei (the coil-globule transition). In Ref. [6], it was shown that this scenario is valid for the Stockmayer model, which supplements the model of dipolar spheres with a short-range isotropic attraction between particles. Nevertheless, the problem of the coil-globule transition in dipolar sphere systems without dispersive attraction remains controversial, as well as a closely related phase separation problem.

Irrespective of their influence on the MF physical properties, chains of magnetic nanoparticles are of considerable independent interest, because they offer much promise for various fields, such as micromechanical sensors, recording media, and drug delivery [28]. Researchers' interest here is not only with the chains formed under the action of the external fields and/or dipole-dipole interactions but also with the chains, which integrity and structure are maintained by nonmagnetic forces. The latter include magnetosome chains of magnetotactic bacteria [29] and magnetic filaments [30–32].

In this paper, we investigate the equilibrium conformation and magnetic structure of a single chain of dipolar hard spheres in zero magnetic field. We focus our attention on two variants: rigid rodlike and flexible chains. In the first case, particle

centers are immovably fixed on one axis, but their magnetic moments retain orientational freedom. In the second case, particles are able to move in the three-dimensional space but with a severe restriction: the distance between centers of the first-nearest neighbors never exceeds a given limiting value. We consider this value as an independent parameter. The problem is solved by means of Langevin molecular dynamics simulations.

II. MODEL DESCRIPTION AND SIMULATION DETAILS

Several approaches are used in literature to define a chain of dipolar spheres. Spatial or energy criteria as well as their combination might be employed to determine whether the particle belongs to a chainlike aggregate [4,5,20,24,27]. The simplest spatial criterion is based on the proximity of bonded particles. Specifically, it says that the distance between neighboring particles in chain should be no more than some critical value $r_{\max}$. In our study, we force the system to fulfill this criterion. This can be interpreted as if the centers of the first-nearest neighbors were permanently linked by flexible inextensible threads of length $r_{\max}$. Thus, the simulated chain consists of N sequentially connected spherical particles of diameter d and magnetic moment $\boldsymbol{\mu}$. The total potential energy of the ith particle is

$$U_i = \sum_{\substack{j=1 \\ j\neq i}}^{N} \left[u^{sr}(r_{ij}) + u_{ij}^{dd}\right] + u_i^{\text{bond}+} + u_i^{\text{bond}-}, \qquad (1)$$

where $\boldsymbol{r}_{ij} = \boldsymbol{r}_i - \boldsymbol{r}_j$ is the interparticle separation vector, u_{ij}^{dd} is the dipole-dipole potential, $u^{sr}(r)$ is the short-range steric repulsion potential, and $u_i^{\text{bond}\pm}$ is the additional bonding potential, which keeps neighboring particles close to each other and maintains the chain integrity:

$$u_{ij}^{dd} = \frac{\mu_0}{4\pi}\left(\frac{\boldsymbol{\mu}_i\cdot\boldsymbol{\mu}_j}{r_{ij}^3} - \frac{3(\boldsymbol{\mu}_i\cdot\boldsymbol{r}_{ij})(\boldsymbol{\mu}_j\cdot\boldsymbol{r}_{ij})}{r_{ij}^5}\right), \qquad (2)$$

where μ_0 is the vacuum permeability. In molecular dynamics, the potential of steric repulsion is conventionally represented by the truncated and shifted Lennard-Jones 12-6 potential. But in order to closely approach the true hard sphere repulsion we use the expression

$$u^{sr}(r) = \begin{cases} 4k_BT\left[\left(\frac{d}{r}\right)^{48} - \left(\frac{d}{r}\right)^{24} + \frac{1}{4}\right], & r < 2^{1/24}d \\ 0, & r \geqslant 2^{1/24}d \end{cases}, \qquad (3)$$

where k_B is Boltzmann's constant and T is the temperature. Additional comments on this choice of the steric repulsion potential are given in Sec. IV. We define the bonding potential as

$$u_i^{\text{bond}\pm} = u^{sr}(r_{\max} + d - r_{i,i\pm1}), \qquad (4)$$

additionally assuming that $u_1^{\text{bond}-} = u_N^{\text{bond}+} = 0$ (chain ends are free).

The Langevin equations of motion for the ith particle are given by [7,33]

$$m\dot{\boldsymbol{v}}_i = -\nabla U_i - \gamma^T\boldsymbol{v}_i + \boldsymbol{\zeta}_i^T, \qquad (5)$$

$$J\dot{\boldsymbol{\omega}}_i = -\boldsymbol{\mu}_i \times \frac{\partial U_i}{\partial \boldsymbol{\mu}_i} - \gamma^R\boldsymbol{\omega}_i + \boldsymbol{\zeta}_i^R, \qquad (6)$$

where m is the particle mass, J is its moment of inertia, $\boldsymbol{v}_i$ and $\boldsymbol{\omega}_i$ are linear and angular velocities, respectively, γ^T and γ^R are translational and rotational friction coefficients, and $\boldsymbol{\zeta}_i^T$ and $\boldsymbol{\zeta}_i^R$ are the Gaussian random force and torque, which satisfy the conditions $\langle\zeta_{il}^{T(R)}(t)\rangle = 0$ and $\langle\zeta_{il}^{T(R)}(t_1)\zeta_{jk}^{T(R)}(t_2)\rangle = 2\gamma^{T(R)}k_BT\delta_{lk}\delta_{ij}\delta(t_1-t_2)$, where k and l denote the vector components. Equations of motion are used in the dimensionless form in a way similar to Ref. [7]. We use m as a unit of mass, d as a unit of length, k_BT as unit of energy, and $\sqrt{4\pi d^3k_BT/\mu_0}$ as a unit of magnetic moment. Hence, md^2 is a unit of moment of inertia, $\sqrt{mk_BT/d^2}$ is a unit of translational friction coefficient, $\sqrt{mk_BTd^2}$ is a unit of rotational friction coefficient, and $\sqrt{md^2/k_BT}$ is a unit of time. In what follows, x^* denotes quantity x measured in corresponding reduced units. Equations (5) and (6) are integrated using the modified leapfrog-Verlet algorithm proposed by Grønbech-Jensen and Farago [34]. Typical simulation parameters are $J^* = 0.1$, $\gamma^{*T} = 1$, $\gamma^{*R} = 1$, and the time step is $\Delta t^* = 0.002$.

The input parameters of the problem are the chain length N, the dipolar coupling constant $\lambda = (\mu_0/4\pi)\mu^2/d^3k_BT = \mu^{*2}$, and the "bond length" $r_{\max}^*$. Coupling constant determines the strength of dipole-dipole interactions in the system and controls values of the first terms in the right-hand side (RHS) of Eqs. (5) and (6). The "bond length" can vary over a wide range of values starting from $r_{\max}^* = 1$. It is obvious that the limiting case $r_{\max}^* \to \infty$ corresponds to the system of free dipoles with infinitesimal concentration. In Sec. IV we also pay special attention to the condition $r_{\max}^* = (2\lambda)^{1/3}$ introduced in Ref. [20]. This condition corresponds to the maximum distance between neighboring particles, at which their dipolar potential in the "head-to-tail" configuration still exceeds thermal energy. Simulations are performed using open boundary conditions, and all interparticle interactions are calculated directly (the all-pairs approach).

III. RIGID RODLIKE CHAIN

Early theoretical studies on chains in MF [12–14] often ignored chain flexibility as they were carried out in the limit $\lambda \gg 1$. It was assumed that in this case chains are close to saturation, when all dipole moments are oriented along the chain axis in the "head-to-tail" manner. Further investigations showed that even consideration of small deviations from the rodlike configuration is important for an accurate description of dipolar systems properties [17]. Furthermore, at low concentrations long chains tend to form rings [24,35]. Nonetheless, in this section we consider a stiff rodlike chain under the assumption that the rod configuration results from some auxiliary external factors (similar to how it was done in Ref. [36]). Such an approach can hardly apply to a quantitative description of aggregates in MF, but it allows a more complete understanding of orientational transitions in polar nanosystems.

At the start of each simulation, particle centers are positioned along the Cartesian z axis ("chain axis"), the distance between neighbors is equal to the particle diameter (i.e., $r_{\max}^* = 1$). Initial orientations of dipole moments are random, unless otherwise specified. During the simulation, particle translational degrees of freedom are eliminated and Eq. (5)

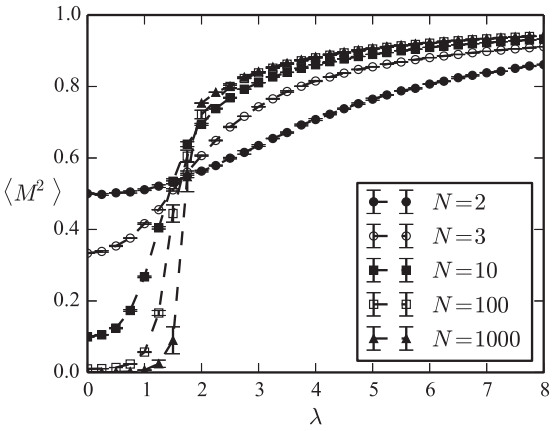

FIG. 1. Mean squared magnetic moment $\langle M^2 \rangle$ as a function of the coupling constant λ for rodlike chains of different lengths.

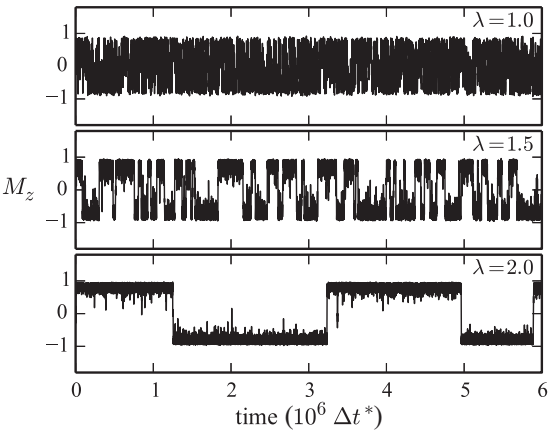

FIG. 2. Fluctuations of the z component of the magnetic moment M_z of rodlike chain at different λ. $N = 10$.

is not used. The state of the chain is characterized by two dimensionless parameters: the mean squared reduced moment $\langle M^2 \rangle = \langle (\sum_{i=1}^{N} \boldsymbol{\mu}_i)^2 \rangle / \mu^2 N^2$, insensitive to possible magnetization reversals, and the z component of the mean reduced moment $\langle M_z \rangle = \langle \sum_{i=1}^{N} \boldsymbol{\mu}_i \rangle / \mu N$, sensitive to magnetization reversals. Their values are averaged over 8×10^6 time steps after 2×10^6 time steps for equilibration.

Obtained results for the mean squared moment at different N and λ are shown in Fig. 1. As one might expect, at small values of the coupling constant ($\lambda \ll 1$) particle moments fluctuate independently and the mean squared moment of the system decreases with increasing N according to the law $\langle M^2 \rangle = 1/N$. An increase of the coupling constant results in the correlation between particles, and at $\lambda \gg 1$ all the moments are aligned along the chain axis, so $\langle M^2 \rangle \simeq 1$. A transition from the chaotic orientation of particle moments to the spontaneous ordering occurs within some range of λ, which diminishes as the chain becomes longer. At $N > 100$ the dependence of $\langle M^2 \rangle$ on λ approaches a steplike behavior, which can be compared to the paramagnetic-ferromagnetic phase transition. It is to be noted, though, that at large coupling constants ($\lambda > 3$) chains of this length are able to go to a long-lived state with two or three magnetic domains of nearly the same size, provided that initial orientations of particle moments were random. Inside each domain dipole moments have the same orientation, but the mean magnetic moments of neighboring domains are antiparallel. The characteristic width of the domain boundary is about a few particle diameters, and its position randomly varies with time. The average internal energy per particle in such a state is only slightly higher than in the case of uniform magnetization, and the lifetime of this state is significantly longer than the typical simulation time. A proper analysis of the domain formation process have not been carried out yet. To prevent domain formation in the current study, we used the saturation configuration as an initial for long chains with $N > 100$.

Interpretation of the simulation results becomes more complicated, if, instead of $\langle M^2 \rangle$, $\langle M_z \rangle$ is chosen as the order parameter (as was done, for example, in Ref. [37]). The fact is that the full magnetic moment $\boldsymbol{M} = \sum_{i=1}^{N} \boldsymbol{\mu}_i / \mu N$ continuously fluctuates: Its z component chaotically changes sign, whereas the absolute value of the moment remains invariant (or almost invariant). As an example, let us refer to Fig. 2, which shows the dynamics of magnetization reversal in the chain consisting of ten particles over 6×10^6 time steps. It is readily seen that the frequency of reversals strongly depends on the coupling constant and changing by two or three orders of magnitude over the range $1 < \lambda < 2$. It means that the answer to the question of whether the chain is in the ordered state depends not only on the coupling constant but also on the time interval, over which the results of simulation are averaged (i.e., on the time of observation). Thus, at $\lambda = 2$ averaging of M_z over the interval of 10^6 time steps gives a positive answer, while averaging over the interval of 10^8 time steps gives a negative answer ($|\langle M_z \rangle| \ll 1$).

To describe quantitatively the dynamics of magnetization reversal we calculated the relative frequency of reversals $\nu(\lambda) = n_{\mathrm{rev}}(\lambda)/n_{\mathrm{rev}}(0)$, where $n_{\mathrm{rev}}(\lambda)$ is the number of simulation steps, accompanied by a change of sign of M_z, over the specified simulation time (10^7 time steps). The dependencies of the frequency on the coupling constant for $\lambda \leqslant 6$ are presented in Fig. 3. It is seen that the chain length is essential

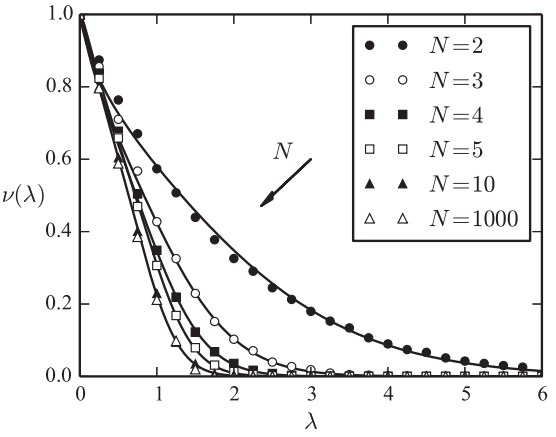

FIG. 3. Relative frequency of magnetization reversals in rodlike chain ν as a function of the coupling constant λ for different chain lengths. Lines are from approximation Eq. (8); points are simulation results.

only at $N < 10$. At $N \geqslant 10$ the results of calculation fall on a single universal curve. This can be explained by the fact that dynamics of each particle in the chain is determined mainly by the finite number of its nearest neighbors. We varied the rotational friction coefficient and the time step in rather broad ranges ($0.1 \leqslant \gamma^{*R} \leqslant 10$, $0.0005 \leqslant \Delta t^* \leqslant 0.004$), but we did not find the somewhat noticeable effect of these parameters on frequency values.

The observed process of magnetization reversal in the rodlike chain is very similar to moment fluctuations in a uniaxial single-domain particle, described by Néel [38]. Energetically favorable orientations of the Néel particle are those where its dipole moment is directed "up" or "down" along the easy magnetization axis. Energy barrier between two states is Kv_0, where K is the constant of magnetic anisotropy and v_0 is the particle volume. The characteristic time τ_N of the particle staying in one of this two states is proportional to $\exp(\sigma)$, where $\sigma = Kv_0/k_BT$ is the reduced barrier height. If the time of observation is much less than τ_N, the Néel relaxation can be neglected and the magnetic moment can be considered frozen in the particle. The situation with chains is alike. The states with $M_z \simeq 1$ and $M_z \simeq -1$ are energetically equivalent, and the probability of spontaneous transition between them decreases drastically with the growth of λ. There exist a conventional interpolation formula for the Néel relaxation time [39,40]:

$$\tau_N(\sigma) = \tau_D \frac{e^\sigma - 1}{2\sigma}\left(\frac{1}{1+1/\sigma}\sqrt{\frac{\sigma}{\pi}} + 2^{-\sigma-1}\right)^{-1}, \quad (7)$$

where τ_D is a reference relaxation time, independent of the anisotropy constant. We tried to fit calculated frequencies with the expression

$$\nu(\lambda) = \tau_D/\tau_N(\tilde{\sigma}(\lambda)), \quad (8)$$

where $\tilde{\sigma}(\lambda) = a\lambda^b$ plays a role of the reduced energy barrier, and a and b are fitting parameters. Values of a and b, obtained by the least squares method, are given in Table I, and fitting results are presented in Fig. 3 as solid lines. The agreement with numerical data is rather good at high coupling constants $\lambda > 1$. Thus, the dynamics of magnetization reversal in the chain of interacting dipoles shows a strong analogy to the Néel relaxation of a single-domain particle with a finite energy of magnetic anisotropy, and the characteristic time of the chain being in the "ferromagnetic" state is described with a good accuracy by Eq. (7) after replacing the anisotropy parameter σ by the quantity $\tilde{\sigma}(\lambda)$.

TABLE I. Fitting parameters of approximation Eq. (8) for the frequency of magnetization reversals in the N-particle rodlike chain.

N	a	b
2	1.17	1.01
3	1.93	1.21
4	2.37	1.37
5	2.60	1.58
10	3.20	1.59

IV. FLEXIBLE 3D CHAIN

The initial configuration of the flexible chain is created by positioning the first particle at the origin of coordinates, and each subsequent ith particle at a random location inside the spherical layer $d \leqslant r_{i,i-1} \leqslant r_{\max}$. The overlap between particles is not allowed. Orientations of magnetic moments are random. Simulation starts with $\lambda = 0$, and every 1.5×10^5 time steps parameter λ is incremented until it reaches the desired value. After this, additional 10^6 steps are used for equilibration and 10^7 steps for data sampling. Besides, for every combination of input parameters the averaging over ten independent realizations with different initial conditions is performed. As was mentioned in Sec. II, when choosing the value of $r^*_{\max}$ we were guided first of all by the criterion $r^*_{\max} = (2\lambda)^{1/3}$ [20]. All results given below are obtained for $r^*_{\max}(\lambda) = \max(1,(2\lambda)^{1/3})$, unless otherwise specified. The range of high coupling constants $4 \leqslant \lambda \leqslant 10$, which is usually associated with phase and structural transformations in three-dimensional (3D) dipolar systems, in this case corresponds to the range of "bond length" $2 \leqslant r^*_{\max} \lesssim 2.7$.

Figure 4 presents the mean squared reduced moment of flexible chains with different lengths as a function of the coupling constant λ. Solid lines are from the analytical expression

$$\langle M^2\rangle = \frac{1}{N} + 2\frac{K}{N^2(1-K)^2}(N - 1 + K^N - NK), \quad (9)$$

where $K = L(\lambda/2)$, $L(x) = \coth(x) - 1/x$ is the Langevin function. Equation (9) was derived in Ref. [17]. It takes into account only interactions between the nearest neighbors and assumes that deviations of the chain from the saturated rodlike configuration are small (i.e., $\lambda \gg 1$). We must note here that using truncated and shifted Lennard-Jones 12-6 potential for steric repulsion, we were not able to achieve a good agreement with Eq. (9) even for $N = 2$: At $\lambda \geqslant 10$ simulation data overestimated theoretical values. On the contrary, as it seen from Fig. 4, with steric potential Eq. (3) simulation data fit the analytical model well for $N = 2,3$ and $\lambda \geqslant 10$. It was the key motivation for us to use Eq. (3) in this work. However,

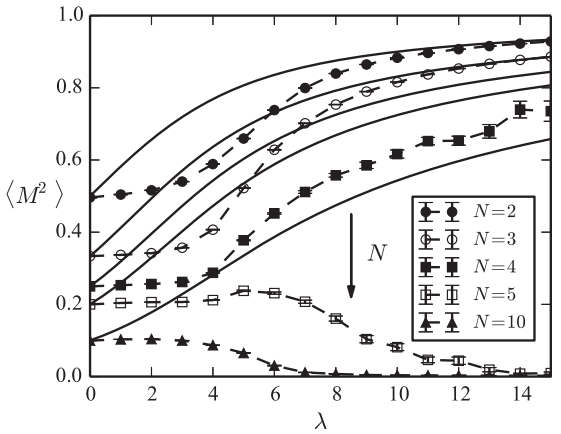

FIG. 4. Mean squared magnetic moment $\langle M^2\rangle$ as a function of the coupling constant λ for flexible chains of different lengths. $r^*_{\max} = \max(1,(2\lambda)^{1/3})$. Solid lines are from the theoretical model by Mendelev and Ivanov [Eq. (9)]; points are simulation results.

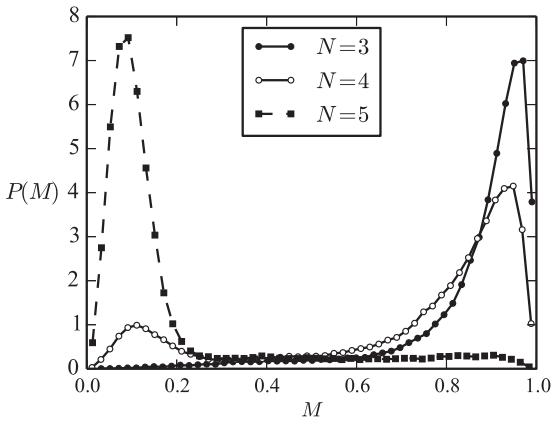

FIG. 5. Probability distributions of the reduced magnetic moment M for flexible chains of different lengths. $\lambda = 10$, $r^*_{\max} = (2\lambda)^{1/3} \simeq 2.7$.

already for $N = 4$ the agreement breaks down. Evidently, this divergence is due to the fact that Eq. (9) does not take into account interactions of non-neighboring particles and the possibility of chain folding into ring. But since at $N \geqslant 4$ the ring configuration is in fact energetically more favorable than the disclosed chain configuration [35,36], the inconsistency of numerical results with theoretical predictions appears to be natural. The importance of taking into account interactions between non-nearest neighbors for correct analytical description of flexible dipolar chains was also emphasized in a recent study Ref. [32].

Flexible chain with $N \geqslant 4$ chaotically jumps between two states, in one of which its reduced magnetic moment is small (chain is closed) and in the other state the moment is close to unity (chain is disclosed). Figure 5 shows distributions of the reduced magnetic moment $M = |\sum_{i=1}^{N} \boldsymbol{\mu}_i|/\mu N$ at $\lambda = 10$. It is seen that for $N = 3$ the most probable configuration is that of the disclosed linear chain with $\langle M \rangle \simeq 0.9$, for $N = 5$ it is the ring with $\langle M \rangle \simeq 0.1$, and for $N = 4$ the distribution has two peaks, i.e., probabilities of ring and chain configurations are comparable.

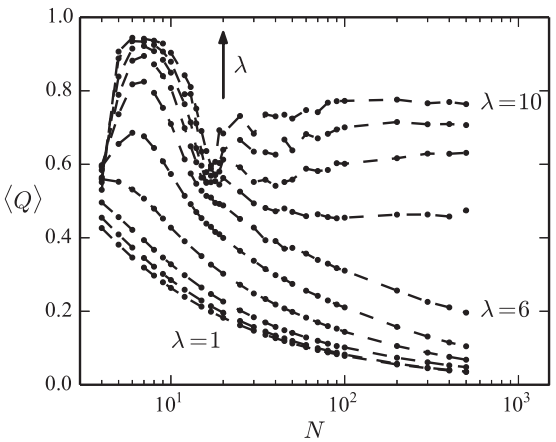

FIG. 6. Mean toroidal moment $\langle Q \rangle$ of the flexible chain as a function of the particle number N at different coupling constants λ. From bottom to top, λ is increased by unity. $r^*_{\max} = (2\lambda)^{1/3}$.

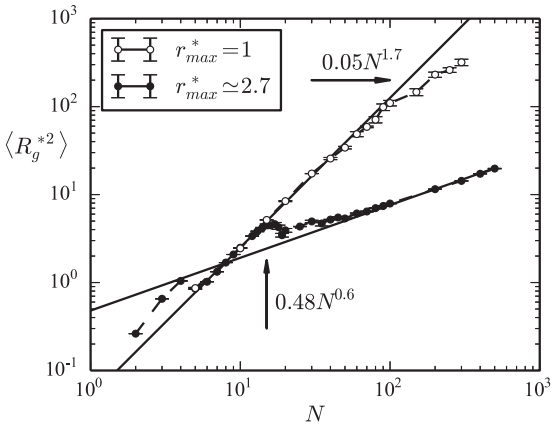

FIG. 7. Mean squared radius of gyration of flexible chains with "strongly bonded" ($r^*_{\max} = 1$) and "weakly bonded" ($r^*_{\max} = (2\lambda)^{1/3} \simeq 2.7$) neighbors vs the chain length N. $\lambda = 10$. Solid lines are power law approximations.

Since for $N > 4$ the reduced magnetic moment tends to zero with increasing λ, the "ferromagnetic" ordering is absent in long chains. As for the azimuthal ordering of magnetic moments, it seems reasonable to choose as the order parameter the reduced toroidal moment $\langle Q \rangle = \langle |\sum_{i=1}^{N} \boldsymbol{r}_i^c \times \boldsymbol{\mu}_i / r_i^c| \rangle / \mu N$, where $\boldsymbol{r}_i^c$ is the particle position relative to the system center of mass. Toroidal moment of a large ideal ring with azimuthal ordering of dipoles is equal to unity.

Figure 6 shows $\langle Q \rangle$ as a function of chain length N. From plots it is evident that at moderate values of the coupling constant ($\lambda \leqslant 4$) toroidal moment of the chain decreases monotonically with the growth of its length, which implies the absence of any magnetic ordering. At larger values of the coupling constant the general picture undergoes qualitative changes: Curves demonstrate the presence of circular order and a nonmonotonic variation of the toroidal moment, as the length increases. For an understanding of this complicated behavior of curves, it will be useful to discuss the question of the chain conformation.

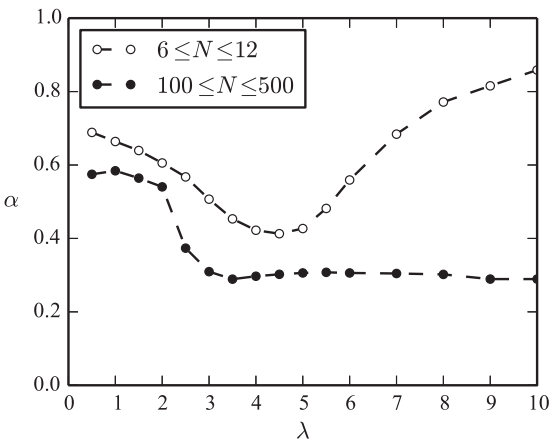

FIG. 8. Inverted cluster dimensionality α [the exponent of the power law Eq. (10)] as a function of the coupling constant λ. α is independently determined for short ($6 \leqslant N \leqslant 12$) and long ($100 \leqslant N \leqslant 500$) flexible chains. $r^*_{\max} = (2\lambda)^{1/3}$.

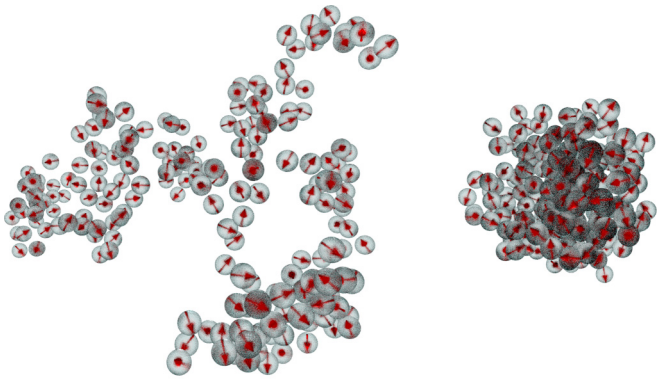

(a) (b)

FIG. 9. (Color online) Snapshots of typical configurations of a long flexible chain at different values of the dipolar coupling constant λ. $N = 200$, $r^*_{\max} = (2\lambda)^{1/3}$. (a) $\lambda = 2$, (b) $\lambda = 4$.

The so-called radius of gyration $R_g^2 = \sum_{i=1}^{N} (\boldsymbol{r}_i^c)^2/N$ is often used to characterize shape and size of particle clusters [31,41]. The dependence of the ensemble-averaged squared radius of gyration on the number of particles in the cluster can be approximated by a power law

$$\langle R_g^2 \rangle \propto N^{2\alpha}, \tag{10}$$

where the exponent α (inverted dimensionality of the cluster) contains information on cluster shape. For the ideal ring $\alpha = 1$, for a compact three-dimensional object $\alpha = 1/3$ and for a self-avoiding random walk $\alpha = 0.6$ [31,41]. The applicability of Eq. (10) for description of dipolar chains is evident from Fig. 7: The results of our calculations in the logarithmic coordinates are fitted by straight lines. Open circles correspond to chains, in which particles closely adjoin each other ($r^*_{\max} = 1$), and black circles correspond to chains containing relatively free particles ($r^*_{\max} = (2\lambda)^{1/3}$). In the first case, most of the results fall on the curve $\langle R_g^{*2} \rangle = 0.05N^{1.7}$, which corresponds to a deformed ring with $\alpha \simeq 0.9$. In the second case, there are two characteristic size ranges. For short chains ($6 \leqslant N \leqslant 12$) α is also about 0.9, and for long chains ($100 \leqslant N \leqslant 500$) $\alpha \simeq 0.3$. The inverted cluster dimensionality as a function of the coupling constant for both of these size ranges is shown in Fig. 8. At small values of the coupling constant all chains are close to a swollen random coil configuration [see Fig. 9(a)]. With increasing coupling constant up to $\lambda \simeq 4$ the parameter α decreases, which is indicative of the formation of dense three-dimensional clusters—quasispherical globules [see Fig. 9(b)]. This conclusion actually agrees with the known analytical predictions of Ref. [20], where interactions between non-nearest neighbors in chain were taking into account in the framework of the concept of "quasimonomers," which treats a long flexible chain as a system of disconnected segments. Based on the estimate of the second viral coefficient of "quasimonomer" ensemble it has been concluded that at $\lambda \simeq 4$ the system undergoes the coil-globule transition. As it seen from Figs. 4 and 6 the reduced magnetic and toroidal moments of spherical globules at this point are rather small and magnetic ordering is absent.

At higher coupling constants equilibrium morphology and magnetic structure markedly depend on the chain length. Examples of equilibrium configurations of flexible chains at high coupling constants are given in Fig. 10. Short chains with $5 \leqslant N < 15$ at $\lambda \gtrsim 6$ are transformed into almost ideal rings with cluster dimensionality and toroidal moments close to unity [see Fig. 10(a)]. Chains with $15 \leqslant N \leqslant 20$ are transformed into deformed rings with lower toroidal moment or into figure-of-eight structures, in which toroidal moments of two loops have different signs and partially compensate each other [see Fig. 10(b)]. As the chain length further increases figures-of-eight structures are replaced by two- and three-loop structures, in which toroidal moments of loops have the same direction [see Fig. 10(c)]. The full toroidal moment rises. This explains a sharp minimum of $\langle Q \rangle$ in Fig. 6. The longest chains ($N \geqslant 100$) at $\lambda \simeq 8$ are transformed into toroidal globules with a circular arrangement of magnetic moments [see Fig. 10(d)].

Our results on the structure of large globules qualitatively agree with some known data for the Stockmayer fluid. Thus, in Ref. [6] globules were observed at $\lambda \simeq 4.5$ and did not have the magnetic ordering. In Ref. [41] large spherical metastable globules were observed at $7 < \lambda < 9$ and they demonstrated circular magnetic ordering. In Ref. [42] the authors predicted that the drop of ferromagnetic liquid undergoes a change in topology from spherical to toroidal.

In our simulations the coil-globule transition takes place when $r^*_{\max} = (2\lambda)^{1/3}$, while severe limitation on the translational degrees of freedom ($r^*_{\max} = 1$) inhibits the globule formation (see Fig. 7). To gain a better understanding of how the particle translational degrees of freedom affect the properties of the system, we calculated the equilibrium configurations of a long chain ($N = 400$) over a wide range of bond length $1 \leqslant r^*_{\max} \leqslant 40$. The squared radius of gyration

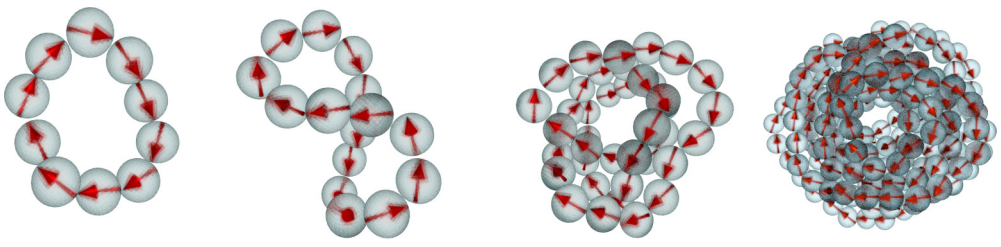

(a) (b) (c) (d)

FIG. 10. (Color online) Snapshots of typical configurations of flexible chains at large coupling constant ($\lambda = 10$) for different numbers of particles N. $r^*_{\max} = (2\lambda)^{1/3} \simeq 2.7$. (a) $N = 10$, (b) $N = 15$, (c) $N = 40$, and (d) $N = 200$.

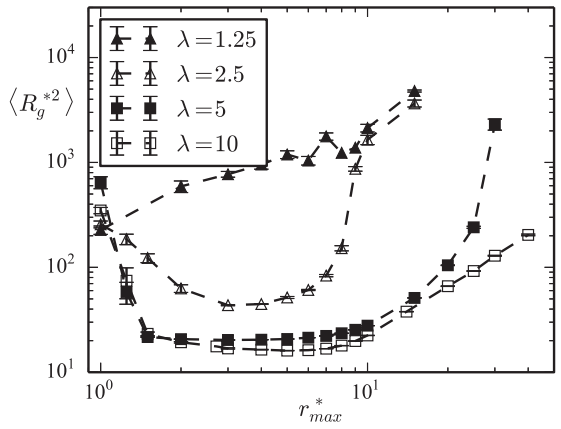

FIG. 11. Mean squared radius of gyration of a long flexible chain as a function of the bond length $r^*_{\max}$ at different coupling constants λ. $N = 400$.

$\langle R_g^2 \rangle$ as a function of $r^*_{\max}$ is presented in Fig. 11. It is seen that the globule state corresponding to $R_g \simeq 5d$ is reached in a rather narrow range $2 \leqslant r^*_{\max} \leqslant 10$. An increase of $r^*_{\max}$ to several dozen destroys the globular state as well as the decrease of $r^*_{\max}$ to unity.

Typical equilibrium chain configurations at different values of $r^*_{\max}$ for large coupling constants are shown in Fig. 12. Flexible chains, in which the neighboring particles are closely pressed to each other ($r^*_{\max} \simeq 1$), transform into the closed loops at $\lambda \gtrsim 6$ and do not show any tendency to form dense three-dimensional clusters [Fig. 12(a)]. This conclusion is consistent with the results of a recent study on magnetic filaments [31], where filaments were treated as chains of magnetic particles held close together by finitely extensible nonlinear elastic (FENE) potential. When $r^*_{\max} > 10$ (i.e., when we approach the limit of the rarefied gas of unbonded dipolar spheres) globules are also absent. In this case, even if a dense cluster is used as an initial configuration, the system rapidly expands [Fig. 12(c)], and breaks down into separate rings with further increase in $r^*_{\max}$ [Fig. 12(d)]. These results agree qualitatively with the known data on the dipolar fluid microstructure [24]. So, the globular state can be reached for long flexible dipolar chains at large values of the coupling constant ($\lambda \geqslant 4$), but only in the limited range of bond length ($2 \leqslant r^*_{\max} \leqslant 10$).

V. CONCLUSION

In the present paper we have investigated equilibrium properties of a single chain of spherical dipoles in a wide range of the dipolar coupling constant λ. Two cases are considered: rodlike and flexible chains.

In the model of the rodlike chain, we exclude translational degrees of freedom of particles, but we do not put any restrictions on orientations of particle dipolar moments. In the absence of dipolar coupling, moments of particles fluctuate independently and the role of magnetization relaxation time in the system is played by the Brownian rotational diffusion time $\tau_B = \gamma^R/2k_BT$. If one wants to take into account the internal magnetic anisotropy of particles, τ_B must be replaced by $\tau = \tau_B\tau_N/(\tau_B + \tau_N)$, where τ_N is the Néel relaxation time of a single particle [40]. Our results show that at $\lambda \gtrsim 1.5$ particles are no longer independent, their moments are chiefly aligned parallel to the chain axis, but magnetization relaxation is still possible as the thermal fluctuations are able to cause spontaneous transition between energetically equivalent states $M_z \simeq 1$ and $M_z \simeq -1$ (magnetization reversal). As dipolar coupling constant grows, such transitions become less probable, the magnetization relaxation time rises, and the frequency of magnetization reversals drops down. This behavior of a linear chain of coupled dipoles is very similar to the Néel relaxation of a single uniaxial magnetic nanoparticle. More than that, the process of magnetization reversal in chain can be successfully described by the formula Eq. (7) for τ_N, after we replace the anisotropy barrier σ with the quantity $\tilde{\sigma}(\lambda) = a\lambda^b$, where a and b are dimensionless parameters of the order of unity, which depend on the system size.

In the model of the flexible chain, particles are able to move in the three-dimensional space, but the distance between centers of the first-nearest neighbors never exceeds a given limiting value $r_{\max}$. For $r_{\max} \simeq d$ chains of five or more particles form stable closed rings at $\lambda \gtrsim 6$. In the case $r_{\max} \geqslant 2d$ the situation is qualitatively different for long chains: At $\lambda \simeq 4$ chains with $N \geqslant 100$ collapse into magnetically unstructured quasispherical globules, and at $\lambda \simeq 8$ they transform into toroidal globules with a strong azimuthal ordering of magnetic dipoles. At $r_{\max} > 10d$ globules become unstable and break down to form separate rings. We see that the problem parameter $r_{\max}$ plays a crucial role in the formation of globular structures. In our opinion, $r_{\max}$ might be viewed as the amplitude of random walk of particles relative to each

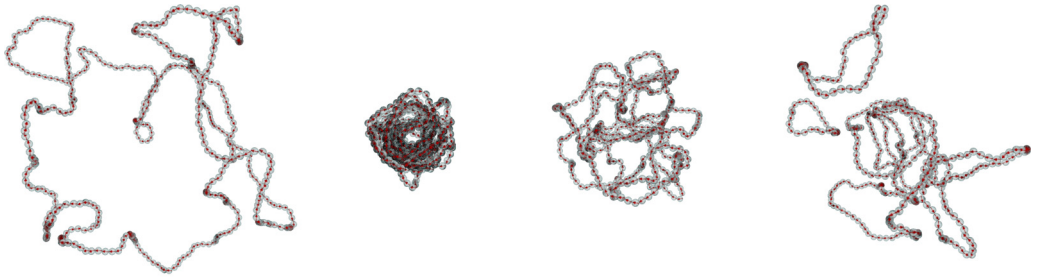

FIG. 12. (Color online) Snapshots of typical configurations of a long flexible chain at large coupling constant ($N = 400$, $\lambda = 10$) for different bond lengths $r^*_{\max}$. (a) $r^*_{\max} = 1$, (b) $r^*_{\max} = 10$, (c) $r^*_{\max} = 20$, and (d) $r^*_{\max} = 30$.

other or as the degree of system extensibility. Flexible but inextensible chain ($r_{max} \simeq d$), where particles are fixed on their positions along the chain and always tightly pressed to their neighbors, are not able to form globular structures. In the other, highly extensible limiting case ($r_{max} > 10d$) particles are able to leave their first-nearest neighbors, the effective interparticle attraction related to magnetodipole interactions weakens, and globular structures become unstable. Thus, the analogy between the coil-globule transition in the flexible chain and the vapor-liquid transition in magnetic fluid manifests itself in a twofold manner. First, the transition in MF is observed in the limited range of average particle concentrations (i.e., in the limited range of average distances between the particles). Second, according to Ref. [27], this transition is observable in simulations of unbonded dipolar hard spheres even without additional attractive potential, if the simulation algorithm takes into account a decrease in the amplitude of random walk of particles in condensed phase.

ACKNOWLEDGMENTS

The work was supported by the Russian Foundation for Basic Research (Grants No. 13-02-00076 and No. 14-01-96007) and by the Ural Branch, Russian Academy of Sciences (Project No. 15-10-1-16). Calculations were performed using the Uran supercomputer of IMM UB RAS.

[1] P. G. de Gennes and P. A. Pincus, Phys. Kondens. Mater. **11**, 189 (1970).
[2] R. Rosman, J. J. M. Janssen, and M. T. Rekveldt, J. Magn. Magn. Mater. **85**, 97 (1990); K. Butter, P. H. H. Bomans, P. M. Frederik, G. J. Vroege, and A. P. Philipse, Nat. Mater. **2**, 88 (2003); A. F. Pshenichnikov and A. A. Fedorenko, J. Magn. Magn. Mater. **292**, 332 (2005); M. Klokkenburg, B. H. Erné, J. D. Meeldijk, A. Wiedenmann, A. V. Petukhov, R. P. A. Dullens, and A. P. Philipse, Phys. Rev. Lett. **97**, 185702 (2006).
[3] J.-M. Caillol, J. Chem. Phys. **98**, 9835 (1993).
[4] J. J. Weis and D. Levesque, Phys. Rev. Lett. **71**, 2729 (1993).
[5] J. M. Tavares, J. J. Weis, and M. M. Telo da Gama, Phys. Rev. E **59**, 4388 (1999).
[6] P. R. ten Wolde, D. W. Oxtoby, and D. Frenkel, J. Chem. Phys. **111**, 4762 (1999).
[7] Z. Wang, C. Holm, and H. W. Müller, Phys. Rev. E **66**, 021405 (2002).
[8] K. Van Workum and J. F. Douglas, Phys. Rev. E **71**, 031502 (2005).
[9] P. C. Scholten, Magn. IEEE Trans. **16**, 221 (1980); S. Taketomi, Jpn. J. Appl. Phys. **22**, 1137 (1983); S. Kamiyama and A. Satoh, J. Colloid Interface Sci. **127**, 173 (1989); S. Odenbach and S. Thurm, in *Ferrofluids*, edited by S. Odenbach, Lecture Notes in Physics Vol. 594 (Springer, Berlin, 2002), pp. 185–201.
[10] P. C. Jordan, Mol. Phys. **25**, 961 (1973).
[11] R. van Roij, Phys. Rev. Lett. **76**, 3348 (1996).
[12] R. P. Sear, Phys. Rev. Lett. **76**, 2310 (1996).
[13] A. Yu. Zubarev and L. Yu. Iskakova, JETP **80**, 857 (1995).
[14] M. A. Osipov, P. I. C. Teixeira, and M. M. Telo da Gama, Phys. Rev. E **54**, 2597 (1996).
[15] A. O. Ivanov and S. S. Kantorovich, Phys. Rev. E **70**, 021401 (2004).
[16] A. O. Ivanov, Z. Wang, and C. Holm, Phys. Rev. E **69**, 031206 (2004).
[17] V. S. Mendelev and A. O. Ivanov, Phys. Rev. E **70**, 051502 (2004).
[18] A. O. Ivanov, S. S. Kantorovich, V. S. Mendelev, and E. S. Pyanzina, J. Magn. Magn. Mater. **300**, e206 (2006).
[19] A. Y. Zubarev and L. Y. Iskakova, Phys. Rev. E **68**, 061203 (2003).
[20] K. I. Morozov and M. I. Shliomis, J. Phys.: Condens. Matter **16**, 3807 (2004).
[21] C. F. Hayes, J. Colloid Interface Sci. **52**, 239 (1975); J. C. Bacri and D. Salin, J. Phys. Lett. **43**, 649 (1982); A. F. Pshenichnikov and I. Yu. Shurubor, Bull. Acad. Sci. USSR, Phys. Ser. **51**, 40 (1987); H. Mamiya, I. Nakatani, and T. Furubayashi, Phys. Rev. Lett. **84**, 6106 (2000).
[22] M. J. Stevens and G. S. Grest, Phys. Rev. Lett. **72**, 3686 (1994).
[23] M. E. van Leeuwen and B. Smit, Phys. Rev. Lett. **71**, 3991 (1993).
[24] L. Rovigatti, J. Russo, and F. Sciortino, Phys. Rev. Lett. **107**, 237801 (2011); Soft Matter **8**, 6310 (2012); S. S. Kantorovich, A. O. Ivanov, L. Rovigatti, J. M. Tavares, and F. Sciortino, Phys. Rev. Lett. **110**, 148306 (2013); L. Rovigatti, S. S. Kantorovich, A. O. Ivanov, J. M. Tavares, and F. Sciortino, J. Chem. Phys. **139**, 134901 (2013).
[25] K.-C. Ng, J. P. Valleau, G. M. Torrie, and G. N. Patey, Mol. Phys. **38**, 781 (1979).
[26] P. J. Camp, J. C. Shelley, and G. N. Patey, Phys. Rev. Lett. **84**, 115 (2000).
[27] A. F. Pshenichnikov and V. V. Mekhonoshin, Eur. Phys. J. E **6**, 399 (2001).
[28] H. Wang, Y. Yu, Y. Sun, and Q. Chen, Nano **6**, 1 (2011).
[29] K. Ērglis, Q. Wen, V. Ose, A. Zeltins, A. Sharipo, P. A. Janmey, and A. Cēbers, Biophys. J. **93**, 1402 (2007); N. A. Usov, M. L. Fdez-Gubieda, and J. M. Barandiarán, J. Appl. Phys. **113**, 023907 (2013).
[30] A. Cebers, J. Phys.: Condens. Matter **15**, S1335 (2003).
[31] P. A. Sánchez, J. J. Cerdà, T. Sintes, and C. Holm, J. Chem. Phys. **139**, 044904 (2013).
[32] P. A. Sánchez, J. J. Cerdà, T. M. Sintes, A. O. Ivanov, and S. S. Kantorovich, Soft Matter **11**, 2963 (2015).
[33] M. P. Allen and D. J. Tildesley, *Computer Simulation of Liquids* (Clarendon Press, Oxford, 1987).
[34] N. Grønbech-Jensen and O. Farago, Mol. Phys. **111**, 983 (2013); N. Grønbech-Jensen, N. R. Hayre, and O. Farago, Comput. Phys. Commun. **185**, 524 (2014).
[35] T. A. Prokopieva, V. A. Danilov, S. S. Kantorovich, and C. Holm, Phys. Rev. E **80**, 031404 (2009).
[36] I. S. Jacobs and C. P. Bean, Phys. Rev. **100**, 1060 (1955).
[37] A. F. Pshenichnikov and A. A. Kuznetsov, Magnetohydrodynamics **49**, 101 (2013).
[38] L. Néel, C. R. Acad. Sci. **228**, 664 (1949); Ann. Geophys. **5**, 99 (1949).

[39] W. T. Coffey, P. J. Cregg, D. S. F. Crothers, J. T. Waldron, and A. W. Wickstead, J. Magn. Magn. Mater. **131**, L301 (1994).
[40] Y. L. Raikher and V. I. Stepanov, J. Magn. Magn. Mater. **368**, 421 (2014).
[41] J. Bartke, Ph.D. thesis, Bergische Universität Wuppertal, 2008 http://nbn-resolving.de/urn:nbn:de:hbz:468-20080158.
[42] S. Banerjee and M. Widom, Brazilian J. Phys. **31**, 360 (2001).